THE JOURNAL OF PHYSICAL CHEMISTRY B

ARTICLE

pubs.acs.org/JPCB

Nonphotochemical Base-Catalyzed Hydroxylation of 2,6-Dichloroquinone by H_2O_2 Occurs by a Radical Mechanism

Stefan Franzen,*[,†] Koroush Sasan,[†] Bradley E. Sturgeon,[§] Blake J. Lyon,[§] Benjamin J. Battenburg,[§] Hanna Gracz,[‡] Rania Dumariah,[†] and Reza Ghiladi[†]

[†]Department of Chemistry, and [‡]Department of Molecular and Structural Biochemistry, North Carolina State University, Raleigh, North Carolina 27695, United States

[§]Department of Chemistry, Monmouth College, Monmouth, Illinois 61462, United States

Supporting Information

ABSTRACT:

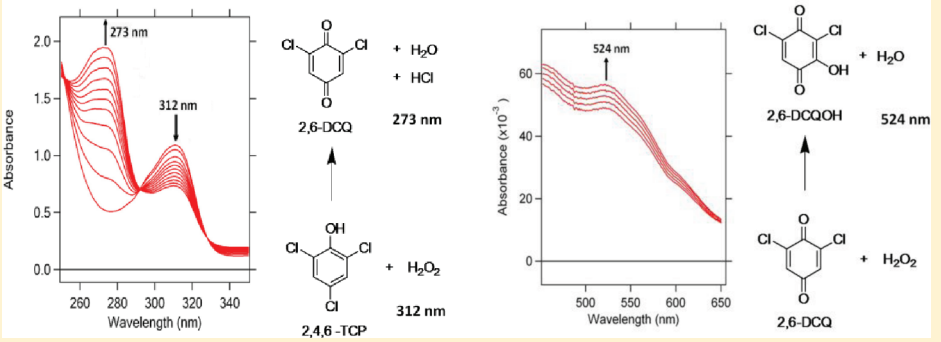

Kinetic and structural studies have shown that peroxidases are capable of the oxidation of 2,4,6-trichlorophenol (2,4,6-TCP) to 2,6-dichloro-1,4-benzoquinone (2,6-DCQ). Further reactions of 2,6-DCQ in the presence of H_2O_2 and OH^- yield 2,6-dichloro-3-hydroxy-1,4-benzoquinone (2,6-DCQOH). The reactions of 2,6-DCQ have been monitored spectroscopically [UV−visible and electron spin resonance (ESR)] and chromatographically. The hydroxylation product, 2,6-DCQOH, has been observed by UV−visible and characterized structurally by ^1H and ^{13}C NMR spectroscopy. The results are consistent with a nonphotochemical base-catalyzed oxidation of 2,6-DCQ at pH > 7. Because H_2O_2 is present in peroxidase reaction mixtures, there is also a potential role for the hydrogen peroxide anion (HOO^-). However, in agreement with previous work, we observe that the nonphotochemical epoxidation by H_2O_2 at pH < 7 is immeasurably slow. Both room-temperature ESR and rapid-freeze-quench ESR methods were used to establish that the dominant nonphotochemical mechanism involves formation of a semiquinone radical (base -catalyzed pathway), rather than epoxidation (direct attack by H_2O_2 at low pH). Analysis of the kinetics using an Arrhenius model permits determination of the activation energy of hydroxylation (E_a = 36 kJ/mol), which is significantly lower than the activation energy of the peroxidase-catalyzed oxidation of 2,4,6-TCP (E_a = 56 kJ/mol). However, the reaction is second order in both 2,6-DCQ and OH^- so that its rate becomes significant above 25 °C due to the increased rate of formation of 2,6-DCQ that feeds the second-order process. The peroxidase used in this study is the dehaloperoxidase-hemoglobin (DHP A) from *Amphitrite ornata*, which is used to study the effect of a catalyst on the reactions. The control experiments and precedents in studies of other peroxidases lead to the conclusion that hydroxylation will be observed following any process that leads to the formation of the 2,6-DCQ at pH > 7, regardless of the catalyst used in the 2,4,6-TCP oxidation reaction.

INTRODUCTION

Several peroxidases have been observed to catalyze the oxidation of 2,4,6-trihalophenols (2,4,6-TXPs) to the corresponding 2,6-dihalo-1,4-benzoquinones (2,6-DXQs).[1−4] The haloquinones, 2,6-DXQs, are quite reactive and can undergo further reactions, which may be both spontaneous and catalyzed in living organisms. We have studied the oxidation of 2,4,6-trichlorophenol (2,4,6-TCP) in the dehaloperoxidase-hemoglobins, DHP A and DHP B, from *Amphitrite ornata*, which serve as a model system for the study of the fate of the product 2,6-DCQ. Although the native substrate of DHP A is believed to be 2,4,6-tribromophenol (2,4,6-TBP), most kinetic studies have been conducted using the more soluble 2,4,6-TCP.[3−6] The reactivity of these two 2,4,6-TXPs is similar. Trichlorophenols are of interest because they are important targets for bioremediation efforts. 2,4,6-TCP is of particular importance because it is ranked number

Received: September 5, 2011
Revised: November 12, 2011
Published: December 07, 2011

21 among the top pollutants registered by the United State Environmental Protection Agency (Appendix A to part 40 of the CFR 423 of EPA regulation).

Although much of the chemistry described in this study is general to peroxidases[1] and even heme proteins in general,[7] we discovered the reactions as part of our research into the structure and function of DHP A. It is therefore useful to briefly introduce the current state of knowledge of DHP A to put the further reactivity of the enzymatic product, 2,6-DCQ, in context. Resonance Raman and NMR studies have shown that 2,4,6-TXPs bind to an external site on DHP, while X-ray crystallography,[8−14] NMR,[15,16] FTIR,[17,18] and Raman[19] have demonstrated that 4-halophenols (4-XPs) bind in a well-defined hydrophobic cavity in the distal pocket above the heme. We have recently shown that 4-XPs are not substrates, as originally proposed,[12] but rather are inhibitors of DHP.[14] On the basis of these studies, it is clear that the mechanism of DHP A and B is similar to the established peroxidase mechanism[20] in that the substrate is oxidized at the surface of the enzyme where it can readily diffuse into solution.[21,22] Thus, it has been suggested that 2,4,6-TXP is oxidized by two one-electron steps rather than a two-electron concerted process.[6,23−27] More recently, we have also proposed that TXP is being oxidized by a single 1-electron peroxidase oxidation of TCP to form TCP$^{\bullet}$, followed by enzyme-independent radical reactions leading to the 2-electron oxidized product.[23]

In the course of enzymatic studies of DHP A, it was observed that a slower secondary process occurred, which consumed the product 2,6-DCQ. Above 20 °C, the DHP A-catalyzed oxidation of 2,4,6-TCP shows a maximum in 2,6-DCQ production (λ_{max} = 273 nm), which then decreases with time as 2,6-DCQ is transformed into one or more secondary products[24] that have not yet been characterized.[4] We noted a similar behavior in the mutant Y38F, which has been studied in detail in the context of radical pathways in the DHP A and B.[4,25,26,28] These observations are similar to the previously reported hydroxylation of quinone products observed using a variety of iron catalysts,[29] in peroxidases,[30,31] and in heme proteins, more generally.[7,32] Iron is not required for the oxidation of 2,4,6-TCP as shown by the oxidation reactions in *Ralstonia eutropha*.[33] Previous reports have shown that both OH^- and HOO^- may play a role in the formation of the semiquinone, which then further reacts to form hydroxylated quinones and other products.[30,34] Understanding secondary product formation in DHP-catalyzed oxidations is important both in a biological context and in bioremediation applications. For example, it is believed that DHP A acts to oxidize 2,4,6-TBP in the coelom of *A. ornata*,[35,36] so the further reactivity of 2,6-DCQ determines the fate of these molecules in benthic ecosystems.[37,38] Moreover, the secondary reactions of 2,4,6-TBP may have an impact on the cellular metabolism in *A. ornata*.[39,40] Haloquinone degradation pathways may involve direct oxidation, for example, epoxidation or radical pathways. Herein, we have applied kinetic, structural, and computational methods to quantitatively understand the secondary reactions, with a specific emphasis on the use of electron spin resonance (ESR) to determine the role of radicals in the reaction pathway. The use of both room-temperature and rapid-freeze-quench (RFQ) ESR spectroscopic methods provides unique electron structural and kinetic information that elucidates the reaction pathways of 2,6-DCQ with greater accuracy than was previously possible.

EXPERIMENTAL SECTION

Sample Preparation. His-tagged DHP A was overexpressed and purified as previously described.[3] The concentration of the protein was determined using the Soret band at 406 nm with a molar absorptivity of 116 400 M^{-1} cm^{-1}.[24] The criterion for purity was that the A_{406}/A_{280} ratio was greater than 4. Purified 6XHis-DHP A was oxidized in the presence of $K_3[Fe(CN)_6]$. Size exclusion chromatography (Sephadex G-25) was used to separate excess $K_3[Fe(CN)_6]$, and the freshly oxidized protein was further purified by ion-exchange chromatography (CM-52) prior to each experiment. For the kinetic assays, the elution buffer was 150 mM KH_2PO_4 buffer at pH 7.0. 2,4,6-Trichlorophenol from Acros Organics was dissolved in 150 mM KH_2PO_4, pH 7 buffer with a final concentration of 3 mM and stored at 4 °C until use. The H_2O_2 solution was diluted from 30% reagent grade H_2O_2 solution (Fisher Scientific) with 150 mM KH_2PO_4, pH 7 buffer to a stock concentration of 17.6 mM. The H_2O_2 solution was prepared freshly before use and stored at 4 °C during the course of a series of experiments.

Kinetic Assays. The kinetic assays were conducted in a 1 cm path length quartz cuvette with a total volume of 1.5 mL. The final concentration of ferric DHP A in the cuvette was $[E]_T \approx 2\ \mu M$, and the 2,4,6-TCP concentration was 300 μM for the kinetic experiments. Spectra were obtained using a photodiode array UV−visible spectrometer (Agilent 8453) equipped with a Peltier temperature controller using benchtop mixing of the reagents. To reach thermal equilibrium, DHP A and 2,4,6-TCP (150 mM KH_2PO_4, pH 7 buffer) were allowed to incubate for 5 min in the thermostatted cuvette. The H_2O_2 solution concentration was 75 times that of DHP A. H_2O_2 was added to the cuvette within 1 s of initiation of data collection.

The data were measured over the wavelength range from 200 to 700 nm with a time sampling rate of 3.1 s. The 2,6-DCQ absorption band (λ_{max} = 273 nm) was monitored as the primary product, with 2,6-DCQOH (524 nm) as the secondary product. The data were analyzed by IgorPro5.0 by fitting the initial rate, which comprised the first 30 s of data collection. The analysis of the Michaelis−Menten kinetics of DHP A has been presented elsewhere.[24]

HPLC/UV−Vis Combined Data Collection. Samples for combined HPLC and UV−visible spectroscopic data collection were prepared by dissolving 100 μM 2,6-DCQ in 1 mL of ethanol and then adding 100 mM potassium phosphate (KP_i) buffer to a total volume of 100 mL, both with and without 200 μM H_2O_2. A sample for HPLC analysis was transferred immediately to the auto sampler vial at the same time the sample was placed in the UV−visible spectrometer. When handled in this manner, the sample was injected onto a C-18 HPLC column ~2 min after preparation. HPLC conditions: mobile phase A = acetonitrile, mobile phase B = 0.1% TFA in pure water and a flow rate of 1 mL/min. A linear gradient from 0 to 30% B was applied for 10 min, followed by a linear gradient from 30 to 100% B for an additional 10 min. UV absorbance measurement was at 273 nm (λ_{max} for 2,6-DCQ).

Room-Temperature ESR Spectroscopy. X-band (~9.8 GHz) ESR spectroscopy was performed using a Bruker EMX spectrometer (Billerica, MA) equipped with a high sensitivity cavity. The samples were prepared by dissolving 0.5 mM 2,6-DCQ with 0.5 mM H_2O_2 at pH 7.4 (100 mM KP_i buffer) introduced into the cavity using the Bruker Aqua-X sample holder.[41] ESR simulations were performed using the WINSIM program.[42] Simulations

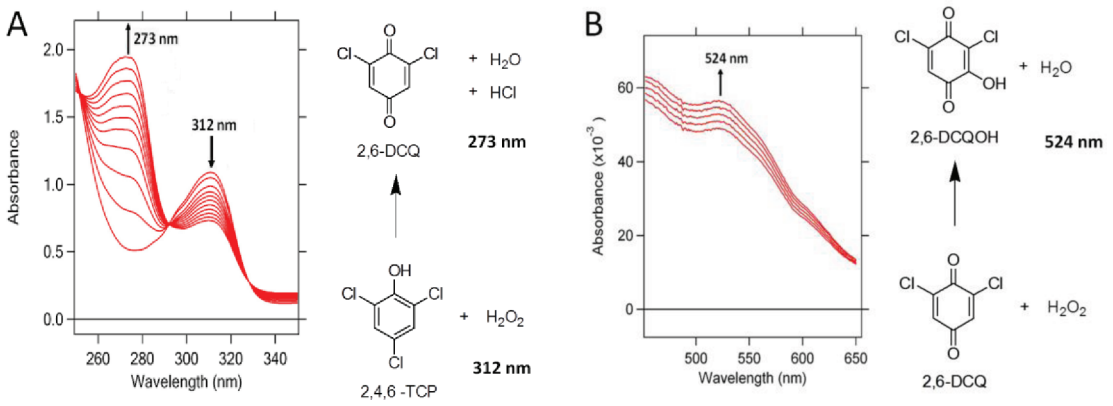

Figure 1. UV−visible spectrophotometric measurement of the DHP-catalyzed oxidation of 2,4,6-TCP. Initial concentrations were [DHP A] ≈ 2 μM, [2,4,6-TCP] ≈ 300 μM, [H_2O_2] ≈ 150 μM, and the assay was conducted at 25 °C in 150 mM KP_i buffer (pH 7). (A) 2,4,6-TCP (312 nm) was converted to the oxidation product, 2,6-DCQ (273 nm). (B) The formation of 2,6-DCQOH (524 nm). The proposed reaction corresponding to the change each of the three absorption bands is shown beside the spectra.

shown use the best-fit parameters as determined by the WINSIM program.

Preparation of Reaction Mixtures by Rapid-Freeze-Quench (RFQ) Methods. DCQ and H_2O_2 solutions were freshly prepared. Prior to each experiment, a stock solution of 20 mM 2,6-DCQ was prepared in ethanol under minimal light conditions. The concentration of H_2O_2 stock solution was determined by measuring its absorbance at 240 nm (ε_{240} = 43.6 M^{-1} cm^{-1}). The stock solutions were then diluted to the appropriate premixing concentration in 100 mM potassium phosphate (0.333 mM H_2O_2, variable pH) or ethanol (1.0 mM 2,6-DCQ) and immediately loaded into the stopped-flow/freeze quench apparatus. Rapid-freeze-quench experiments were performed with a BioLogic SFM 400 freeze-quench apparatus by mixing a 0.333 mM H_2O_2 solution (initial concentration) in 100 mM potassium phosphate (pH 5, 7.4, and 9) with 1.0 mM 2,6-DCQ solution in ethanol at 20 °C using a 3:1 mixing ratio. Reaction times were as follows: pH 5 and pH 7.4, 100 ms, 1 s, and 10 s; pH 9, 20 ms, 1 s, 10 s. For comparative purposes, solutions were also prepared by hand mixing and were quenched at 16 s (pH 7.4) and 13 s (pH 9). A standard 4 mm outside diameter quartz ESR tube was connected to a Teflon funnel, and both the tube and the funnel were completely immersed in an isopentane bath at −110 °C. The reactions were quenched by spraying the mixtures into the cold isopentane, and the frozen material so obtained was packed at the bottom of the quartz tube using a packing rod equipped with a Teflon plunger. Samples were then transferred to a liquid nitrogen storage dewar until they were analyzed.

X-Band ESR Spectroscopy for RFQ Samples. ESR spectra were recorded with an X-band (9 GHz) Varian E-9 ESR spectrometer (Varian, El Palo, CA). Standard 3 mm × 4 mm quartz ESR tubes were used. The temperature of the samples was kept at 190 K for the duration of the data acquisition with a constant flow of nitrogen gas cooled with liquid nitrogen. The flow of the cooled nitrogen gas was adjusted using a Varian temperature controller. The typical spectrometer settings were as follows: field sweep, 100 G; scan rate, 3.33 G/s; modulation frequency, 100 kHz; modulation amplitude, 2.0 G; and microwave power, 2 mW. The exact resonant frequency of each ESR experiment was measured by an EIP-78 (PhaseMatrix, San Jose, CA) in-line microwave frequency counter and is indicated in the figure captions. Typically, 150−200 individual scans were averaged to achieve sufficient signal-to-noise.

NMR Spectroscopy. All of the pulsed field NMR experiments were carried out on a Bruker AVANCE 500 MHz spectrometer (1996) with an Oxford narrow bore magnet (1989), HP XW 4200 host workstation, Topspin software version 1.3. A 5 mm ID 1H/BB (^{109}Ag−^{31}P) triple-axis gradient probe (ID500-5EB, Nalorac Cryogenic Corp.) was used for all measurements. The NMR probe was tuned to the ^{13}C frequency of 125.75 MHz in the 500 MHz spectrometer (^{1}H frequency was 500.128 MHz). The products of hydroxylation of 2,6-DCQ were studied using a combination of homonuclear 2D COSY (^{1}H−^{1}H) and heteronuclear ^{1}H−^{13}C correlated NMR methods. Both 2D heteronuclear single quantum coherence (HSQC) and 2D heteronuclear multiple bond correlation (HMBC) experiments were applied to aid in the assignments. The HSQC experiment measures ^{1}H−^{13}C one bond coupling, and the HMBC experiment measures ^{1}H−^{13}C long-range couplings. Because of the low solubility of 2,6-DCQ in H_2O, the NMR samples were prepared by dissolving 100 mM 2,6-DCQ in ∼0.6 mL of DMSO followed by the transfer of the solution to a 5 mm NMR tube for analysis. Subsequently, ∼0.2 mL of H_2O_2 was added to make a solution with a final concentration of 300 mM H_2O_2 and 100 mM 2,6-DCQ.

DFT Calculations. The generalized gradient approximation of Perdew−Burke−Ernzerhof[43] density functional theory was employed in the ground-state calculations as implemented by the electronic structure package DMol[3,44−47] using a double numeric basis set with one polarization function. Optimized geometries were obtained using the conjugate gradient method constrained to an energy difference of 10^{-6} hartrees. Ground-state calculations implemented both the thermal treatment of electron occupancy[48] with an electronic temperature of 0.02 Ha and the COSMO module employed by DMol[3] (conductor-like screening model), ε = 78.4.[49]

RESULTS

Observation of Spontaneous Reactivity of 2,6-DCQ. The H_2O_2/DHP-catalyzed major oxidation product of 2,4,6-TCP is 2,6-DCQ. Figure 1A shows that the substrate, 2,4,6-TCP (312 nm), was catalytically converted to the product, 2,6-DCQ (273 nm), in the presence of DHP A, following the addition of H_2O_2. However, in these kinetic data, there was also an increase

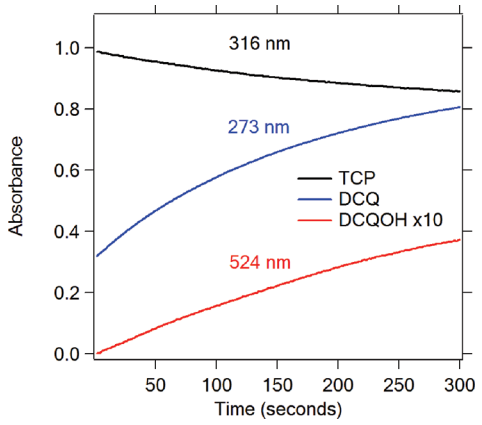

Figure 2. Kinetic trace of 2,4,6-TCP (black trace, 312 nm), 2,6-DCQ (blue trace, 273 nm), and 2,6-DCQOH (red trace, 524 nm) during the oxidation of 2,4,6-TCP with H_2O_2 catalyzed by DHP at 20 °C. Initial concentrations were [DHP A] ≈ 2 μM, [2,4,6-TCP] ≈ 300 μM, [H_2O_2] ≈ 150 μM, and the assay was conducted at 20 °C in 150 mM KP_i buffer (pH 7). The red trace is baseline subtracted for clarity and represents ΔA at 524 nm.

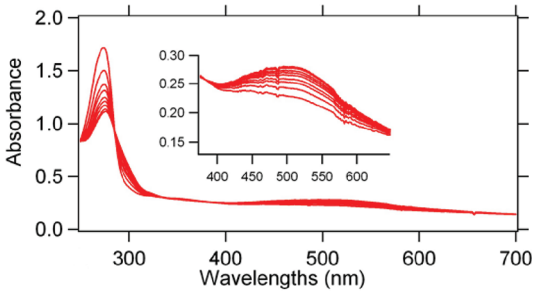

Figure 3. UV−visible spectroscopic measurement of the hydroxylation of 2,6-DCQ (nonenzymatic). The absorbance of 2,6-DCQOH has a maximum at 524 nm. Initial concentrations were [2,6-DCQ] ≈ 150 μM, [H_2O_2] ≈ 150 μM, and the assay was conducted at 25 °C in 100 mM KP_i buffer (pH 7).

in absorbance at 524 nm that has not been investigated in previous studies of DHP (Figure 1B). The observed 524 nm band grows more slowly than the product peak (273 nm) at 20 °C.

The 524 nm band observed in Figure 1B has been previously assigned to a hydroxylated quinone. Specifically, 2,6-DCQ has been observed to convert to 2,6-dichloro-3-hydroxy-1,4-benzoquinone (2,6-DCQOH) in the presence of H_2O_2[34,50−52] in a photochemical, temperature-, and pH-dependent process. A fit to the data in Figure 2 using the method of initial rates gives rates of 9.1×10^{-7} and 1.2×10^{-7} M s^{-1} for the formation of 2,6-DCQ and 2,6-DCQOH, respectively. The analysis is shown in Figure S1 in the Supporting Information. According to previous reports of similar secondary oxidations in peroxidases,[50] we hypothesize that the observed process consists of the hydroxylation of 2,6-DCQ to 2,6-DCQOH. The extinction coefficient of 2,6-DCQOH is 2530 M^{-1} cm^{-1} at 524 nm, which is significantly smaller than the extinction coefficient of 2,6-DCQ (13 200 M^{-1} cm^{-1} at 276 nm).[50] We have observed recently that 2,6-DCQ appears stable below 10 °C, but further reactions take place at temperatures above 10 °C.[24] The absorption band of the secondary product, 2,6-DCQOH (524 nm), was used to study the hydroxylation of 2,6-DCQ in the absence of enzyme. Figure S3 shows that the rate of hydroxylation of 2,6-DCQ was essentially the same in the absence of DHP A as in its presence. Evidence for the spontaneous formation of 2,6-DCQOH is shown in Figure 3, which shows a kinetic trace in the absence of DHP A, but in the presence of 150 μM H_2O_2 at pH 7.

Determination of the Structure of the Hydroxylation Product of 2,6-DCQ. We investigated the hypothesis that 2,6-DCQ is hydroxylated to 2,6-DCQOH by H_2O_2 in aqueous solution using 2D $^1H-^{13}C$ HSQC and 2D $^1H-^{13}C$ HMBC NMR spectroscopic experiments. The aqueous solubility of 2,6-DCQ is too low for NMR studies in D_2O. Consequently, DMSO-d_6 was selected as the solvent. The HMBC experimental data shown in Figure 4A indicated that there are four correlation peaks between protons and carbon atoms in the 2,6-DCQ solution prior to treatment with H_2O_2. These data lead to the conclusion that there are four distinguishable carbons in 2,6-DCQ as expected (Figure 4A). After the addition of ~150 μM H_2O_2 to the 2,6-DCQ solution, six cross-peaks were observed in 2D HMBC spectra, indicating the formation of six distinguishable carbons (Figure 4B). The six peaks can be assigned to the six carbons of 2,6-DCQOH: δ 177 (C_1═O), δ 168 (C_4═O), δ 152 (C_2−OH), δ 122 (C_3−Cl), δ 142 (C_5−Cl), and δ 116 (C_6−H) ppm. There is excellent agreement between the predicted ^{13}C chemical shifts for 2,6-DCQOH[53] and our experimental NMR data (see Table S1). Figure S2 of the Supporting Information shows 2D HSQC data, which exhibit a change in correlation between the hydrogen atoms and carbon atoms 3 and 5 after addition of H_2O_2.

Hydroxylation of 2,6-DCQ Is a Temperature-Dependent Reaction. The activation energy of the rate of oxidation of 2,4,6-TCP by H_2O_2 was determined by the measurement of the temperature dependence of the rate constant.[24] Figure 5 shows that the rate of spontaneous hydroxylation of 2,6-DCQ to 2,6-DCQOH increases with temperature as well. The effect of this spontaneous hydroxylation on the concentration of the 2,6-DCQ product becomes evident above 25 °C at pH 7 for w.t. DHP A. Figure 6 provides an explanation for this observation. The spontaneous rate of formation of 2,6-DCQOH increases with temperature more rapidly than does 2,6-DCQ formation. The kinetics of the 2,6-DCQ product has a biexponential form above 20 °C, which results from an increase in ΔA due to 2,6-DCQ formation followed by a decrease in ΔA due to its conversion to 2,6-DCQOH observed for the 273 nm data in Figure 6. This biexponential behavior and the fit to the data are presented in Figure S4 of the Supporting Information. The model function, $P_1(t) = A_1[1 - \exp(-k_1 t)] - A_2 \exp(-k_2 t)$, has a rapid process, k_1, that leads to 2,6-DCQ formation, and a slower hydroxylation process, k_2, with values $k_1 = 1.8 \times 10^{-2}$ s^{-1} and $k_2 = 3.3 \times 10^{-3}$ s^{-1}, respectively. These values are comparable to the rate constants obtained independently from a fit to substrate decay at 312 nm, $S(t) = A_3 \exp(-k_1 t)$, and growth of the secondary product, P_2, at 524 nm, $P_2(t) = A_4(1 - \exp(-k_2 t))$, as shown in Figures S4 and S5 in the Supporting Information and are confirmed by the method of initial rates in Figure S1 (see analysis in the Supporting Information). Thus, the present study confirms that the hydroxylation of 2,6-DCQ is about 8 times slower than its catalytic formation under the standard conditions used in enzymatic assays ([DHP A] ≈ 2.4 μM, [H_2O_2] < 1.5 mM, [2,4,6-TCP] < 1.5 mM).The fact that the formation of 2,6-DCQOH is ~8 times slower than 2,6-DCQ formation validates the assumption made in the determination of activation parameters for 2,6-DCQ formation in a previous study.[24] The exponential model was necessary because of the

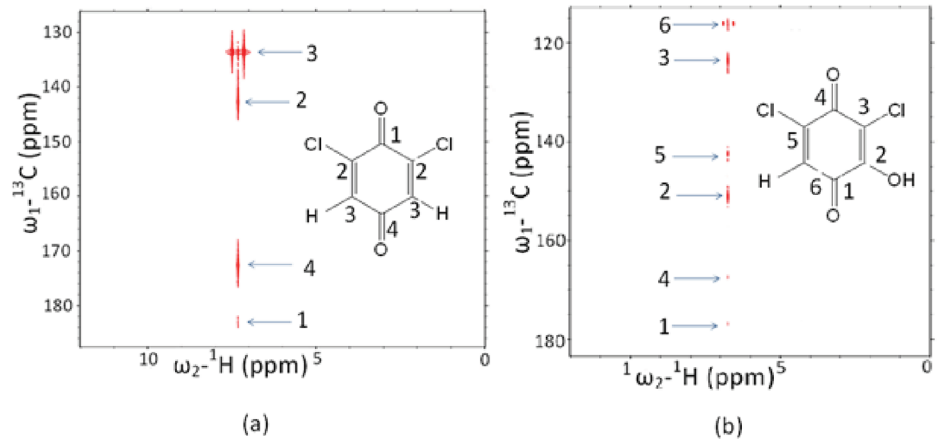

Figure 4. HMBC data obtained on 2,6-DCQ and 2,6-DCQOH in DMSO-d_6. (A) The correlations between the identical H atoms (on C3 and C3′) and all C atoms of 2,6-DCQ are shown. (B) Data obtained on 2,6-DCQOH indicate six different C atoms that are correlated with the single H atom on C-6.

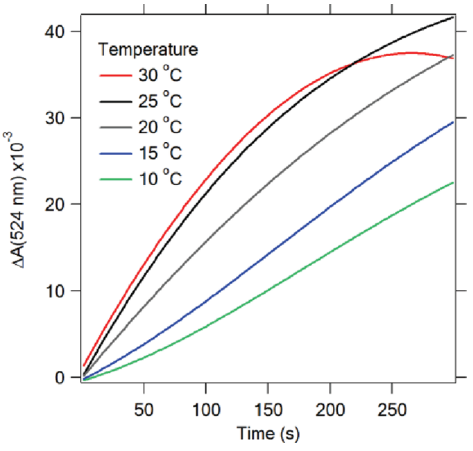

Figure 5. Kinetic traces of 2,6-DCQOH formed during the reaction of 2,4,6-TCP with H_2O_2 as catalyzed by DHP A at 10, 15, 20, 25, and 30 °C. Initial concentrations were [DHP A] ≈ 2 μM, [2,4,6-TCP] ≈ 300 μM, [H_2O_2] ≈ 150 μM, and the assay was conducted in 150 mM KP_i buffer at pH 7.

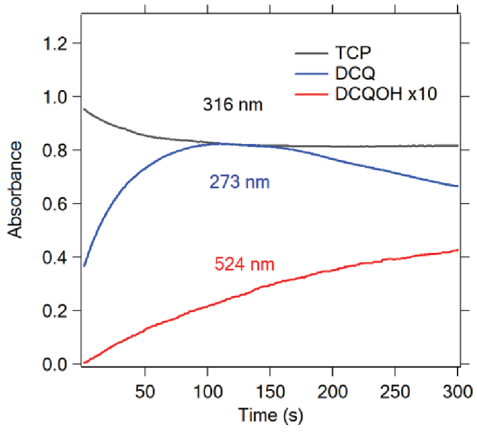

Figure 6. Kinetic trace of 2,4,6-TCP (black trace, 312 nm), 2,6-DCQ (blue trace, 273 nm), and 2,6-DCQOH (red trace, 524 nm) during the oxidation of 2,4,6-TCP with H_2O_2 as catalyzed by DHP A. Initial concentrations were [DHP A] ≈ 2 μM, [2,4,6-TCP] ≈ 300 μM, [H_2O_2] ≈ 150 μM, and the assay was conducted at 25 °C in 150 mM KP_i buffer (pH 7). The red trace is baseline subtracted for clarity and represents ΔA at 524 nm.

biphasic appearance of the data in Figure 6, which was analyzed in Figures S4 and S5. However, the conclusion that the rate constant for formation of 2,6-DCQOH is approximately 8 times less than that for 2,6-DCQ under typical conditions for enzymatic conversion was also verified using the short time approximation, that is, with a linear fit to the data in the first 15 s of the kinetic trace. Linear fits were used for the temperature dependence of the formation of 2,6-DCQOH presented in Figure 5. The fit shown in Figure S7 to the linearized form of the Arrhenius rate constant, $\ln k = -E_a/RT + \ln A$, gives an activation energy of E_a = 36.3 kJ/mol. The details of the analysis are given in Figure S6 and Table S2 of the Supporting Information. It is possible that other products are formed above 30 °C given the observation that the 2,6-DCQOH absorption band at 524 nm begins to level off at the higher temperatures as shown in Figure 5.

Effect of pH on the Hydroxylation of 2,6-DCQ. Most enzymes are sensitive to pH and have specific ranges of activity. A change in pH can protonate or deprotonate an amino acid side group, thereby changing the reactivity of the enzyme.[54−58] Oxidation of TCP as catalyzed by DHP has been studied in the pH range from 4 to 10. The studies showed that changing pH can cause a significant change in the rate of TCP oxidation.[4] DHP shows the highest activity between pH 6.5 and 7.5. To understand the effect of pH on secondary product formation, we studied the degradation of 2,6-DCQ at pH 6.2, 7.4, and 9.0 in the presence and absence of H_2O_2, following the 2,6-DCQ peak by both UV−visible spectroscopy and HPLC. On the basis of the data shown in Figure 7, 2,6-DCQ reacts completely with H_2O_2 in ∼2 min at pH 9.0, but 2,6-DCQ reacts more slowly with H_2O_2 at lower pH. The single exponential time constant is ∼10 min at pH 7.4, but less than <1 min at pH 9.0.

Mechanism of Hydroxylation of 2,6-DCQ. To determine whether there is a radical mechanism for the hydroxylation of 2,6-DCQ, a solution of 2,6-DCQ/H_2O_2 was subjected to room-temperature ESR analysis (Figure 8). When a sample containing 2,6-DCQ/H_2O_2 at pH 7.4 was aspirated into the ESR spectrometer, semistable radical signals (a^H = 2.38 G and a^H = 2.23 G) were observed immediately (Figure 8A) and decayed within ∼3 min. A radical was not observed at pH 6 or 9.0. Scheme 1 provides a

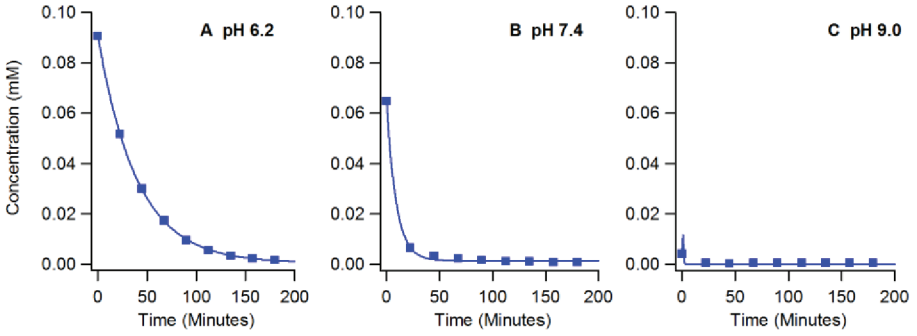

Figure 7. HPLC measurements of the nonenzymatic reaction of 2,6-DCQ with H_2O_2 at (A) pH 6.2, (B) 7.4, and (C) 9.0 (25 °C). Initial concentrations were [2,6-DCQ] ≈ 100 μM, [H_2O_2] ≈ 200 μM.

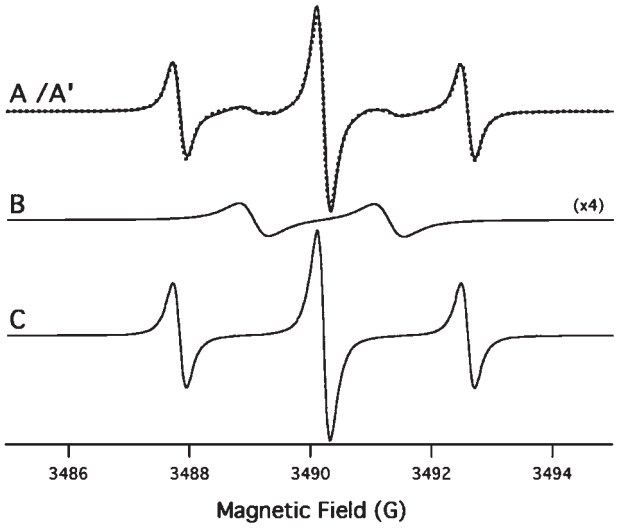

Figure 8. ESR spectrum of semiquinone detected when 2,6-DCQ was mixed with H_2O_2 at pH 7.4. (A, solid line) The ESR spectrum detected when 0.5 mM 2,6-DCQ was mixed with 0.5 mM H_2O_2 and rapidly transferred (~1 min after mixing) to the ESR spectrometer. ESR conditions: 9.80 GHz microwave frequency, 10 mW microwave power, 0.2 G_{PP} modulation amplitude, and a single scan of 81 s/conversion time 164 ms. (A, dashed line) Simulation of (A) using two radical species. Species 1 (81%), 2 spin 1/2 with a^H = 2.38 G; and species 2 (19%), 1 spin 1/2 with a^H = 2.23 G. (B) Simulation of species 2 alone (4× amplitude). (C) Simulation of species 1 alone.

possible mechanism for the formation of hydroxylated secondary products from 2,6-DCQ in the presence of H_2O_2, OH^-, and OOH^-, corresponding to low, intermediate, and high pH, respectively. At low pH, 2,6-DCQOH has been observed to form by electrophilic addition by H_2O_2 via either an epoxide or a cis diol intermediate by a photochemical mechanism. Thus, at low pH, 2,6-DCQOH does not result in the formation of radical intermediates. In addition, 3-dihydroxy-6-chloroquinone (CQ-DiOH) is formed as a side product by HCl elimination. At intermediate pH of 7.4, the reaction is catalyzed by OH^-. 2,6-Dichloro-3-hydroxyhydroquinone dianion (HQ2) is formed by nucleophilic attack by OH^- with further base catalysis by O_2H^- or OH^- to form radical intermediates. At pH 7.4, radical semiquinones SQ1 and SQ2 are formed by reaction of 2,6-DCQ and HQ2. The ESR data indicate that the primary semiquinone is a symmetric radical with two equivalent protons (a^H = 2.38) (SQ1, species 1, Figure 8C), whereas the secondary semiquinone has a single proton (a^H = 2.23) (SQ2, species 2, Figure 8B). We can also consider a termination reaction shown in Scheme 3 that removes 2,6-dichlorohydroquinone dianion (HQ1) by reaction with H_2O_2 (Table 1). It is also possible that 2,6-dichlorohydroquinone reacts with O_2.[30] SQ1 dismutation (2SQ1 → HQ1 + 2,6-DCQ) shown in the bottom row of Scheme 2 is a dominant reaction in solution, at least initially, because 2,6-DCQ has a higher concentration than that of 2,6-DCQOH. If the concentration of 2,6-DCQOH surpasses that of 2,6-DCQ, then SQ2 dismutation (2SQ2 → HQ2 + 2,6-DCQOH) would be the radical termination step (reaction not shown in Scheme 2). Scheme 3 indicates the likely fate of HQ1 in a reaction with H_2O_2, although there may be competing radical reactions to form peroxyl or hydroxyl radicals that are not considered here. An analogous reaction exists for HQ2 (i.e., HQ2 + H_2O_2 → 2,6-DCQOH + $2OH^-$), with similar energetics of $\Delta G^\circ \approx -26.4$ kJ/mol. At pH 9.0, base catalysis leads to an acceleration in the formation of HQ2, which makes it likely that the entire reaction proceeds too rapidly for detection using the room temperature ESR. This observation is consistent with the dramatic increase in rate constant observed by HPLC and would explain why no radicals are observed by room-temperature ESR at pH 9.

RFQ ESR spectra were obtained at pH 5, 7, and 9 to further test the nonphotochemical mechanism of 2,6-DCQ hydroxylation. No signal was observed at pH 5 in either the presence or the absence of H_2O_2 at any quench time examined (up to 10 s), consistent with the results obtained from the room-temperature ESR experiment. At pH 7, the reaction of 2,6-DCQ with H_2O_2 led to the observation of a radical signal at 100 ms that is best described as an anisotropic singlet with a g_{eff} = 2.0064 (Figure 9A). The signal exhibited no time-dependent changes in the shape of the spectral features between the 100 ms, 1 s, and 10 s data (only subtle changes in signal intensity were noted, which were attributed to the differences in packing the ESR tube under RFQ conditions), suggesting that the chemical nature of the radical remained unchanged over the entire time range examined.

In contrast to the room-temperature ESR experiment, the reaction of 2,6-DCQ with H_2O_2 also yielded an observable radical at pH 9, with a g_{eff} = 2.0067 (Figure 9B). Although not quantified, the signal intensity at pH 9 was qualitatively greater than that observed at pH 7.4. Again, no time-dependent changes in the shape of this radical signal were noted between the 20 ms, 1 s, and 10 s data. Overall, the shape and position of the radical signals obtained at pH 7.4 and 9 were virtually indistinguishable, strongly suggesting that the chemical identity of the radical was the same regardless of pH. However, the rise of the signal at pH 9 is

Scheme 1. Mechanism of Hydroxylation of 2,6-DCQ at Low, Intermediate, and High pH[a]

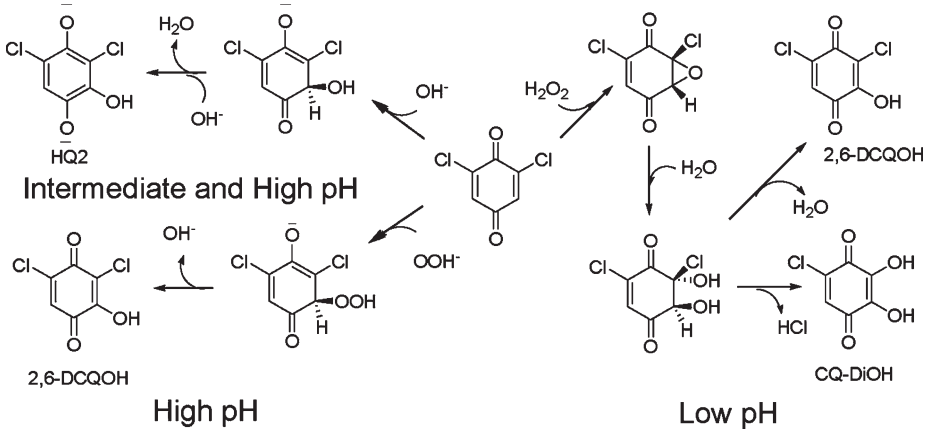

[a] The low pH mechanism has been shown to be a viable photochemical pathway,[5,6] but has negligible rate under nonphotochemical conditions. The intermediate and high pH reactivities are observed at pH 7.4 and 9, respectively.

Scheme 2. Radical Intermediates in the Formation of Hydroxylated Chloroquinones[a]

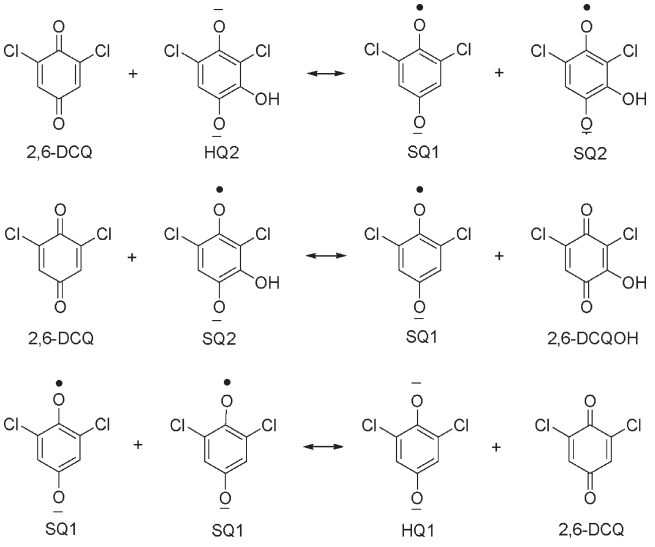

[a] SQ1 and SQ2 are formed from the reaction of 2,6-DCQ and HQ2 at pH 7.4, which we have called intermediate pH in Scheme 1. Two SQ1 radicals can also disproportionate to form 2,6-DCQ and HQ1. The net effect of the radical pathway is to form 2,6-DCQOH as the thermodynamic product.

Scheme 3. Recycling Step for the 2,6-DCHQ Formed during the Radical Chemistry Steps Shown in Scheme [2] To Reform 2,6-DCQ[a]

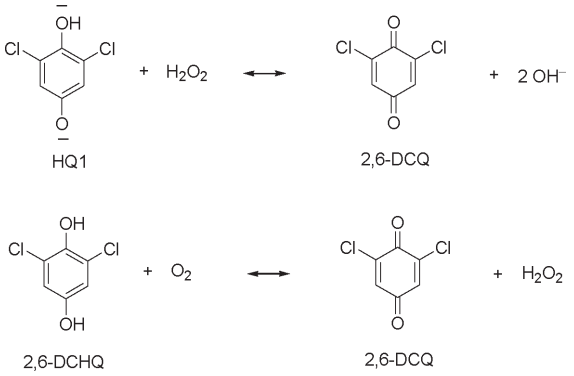

[a] Because O_2 is present in the reaction mixture, we include the reduction of O_2 to H_2O_2, which is a known pathway for oxidation of hydroquinones.

indicative of an increased rate consistent with the hypothesis of base catalysis.

DFT Calculations. We have employed DFT calculations to determine the plausibility of the reaction pathways in Scheme 1 by calculating the change in Gibbs free energy for each step. Ground-state calculations implemented both the thermal treatment of electron occupancy[59] extrapolated to 0 K, and the COSMO module (conductor-like screening model) employed by DMol.[3,49,60] Table 1 divides the possible reactions into base-catalyzed reactions at intermediate and high pH (>7.0) and H_2O_2 epoxidation at low pH (<7.0). The overall free energy change of the hydroxylation of 2,6-DCQ by H_2O_2 is calculated to be ΔG^o = +8.0 kJ/mol. This positive free energy change may arise from the absence of an explicit solvent in the calculation. There is also an error of ~4 kJ/mol for the method. The value of the calculations is to identify high energy intermediates, which have energies far outside the error of the method. The base -atalyzed pathway involves the reaction of OH^- with 2,6-DCQ to form the hydroxyl anion in the 3 position (2,6-DCQ-3-O^-) anion with a free energy change of ΔG^o = 41.0 kJ/mol. Because this high energy species is formed on the pathway, and not directly observed, the free energy change for its formation is the barrier for the reaction and should be comparable to the activation energy, which was measured as E_a = 36 kJ/mol. Subsequently, 2,6-DCQ-3-O^- anion react with either OH^- or O_2H^- to form HQ2 with ΔG^o = −5.4 and −1.2 kJ/mol, respectively (Table 1). The DFT calculation corresponding to the low pH reactivity shows that H_2O_2 attack on 2,6-DCQ leads to formation of 2,6-DCQ epoxide, with $\Delta G^o_{DCQ\ Epox}$ = +8.4 kJ/mol. The epoxide can react further with H_2O to yield 3,5-dichloro-2,3-dihydroxy-1, 4-benzoquinone (2,6-DCQ diOH) with a free energy of $\Delta G^o_{DCQ\ DiOH}$ = +43.9 kJ/mol, which is thus a high energy intermediate along the low pH reaction pathway. There are two

Table 1. Calculated Free Energy for Each Step in the Hydroxylation of 2,6-DCQ[a]

reaction	G° (kJ/mol)	ΔG° (kJ/mol)
Nucleophilic Attack (Base-Catalyzed Pathway)		
2,6-DCQ + OH^- → 2,6-DCQ-3-O^-	−135.1 → −94.1	+41.0
2,6-DCQ-3-O^- + OH^- → HQ2 + H_2O	−136.8 → −142.3	−5.4
2,6-DCQ-3-O^- + O_2H^- → HQ2 + H_2O_2	−151.5 → −152.7	−1.2
HQ2 + 2,6-DCQ → SQ1 + SQ2	−186.6 → −185.4	+1.2
SQ2 + 2,6-DCQ → SQ1 + 2,6-DCQOH	−186.1 → −186.1	0.0
HQ1 + H_2O_2 → 2,6-DCQ + $2OH^-$	−151.0 → −177.8	−26.4
2,6-DCQ + H_2O_2 → 2,6-DCQOH + H_2O	−150.9 → −143.0	+8.0
Formation of Epoxide and Cis Diol by H_2O_2 Addition		
2,6-DCQ + H_2O_2 → 2,6-DCQ epoxide + H_2O	−151.4 → −143.1	+8.4
2,6-DCQ epoxide + H_2O → 2,6-DCQ-diOH	−143.1 → −99.1	+43.9
2,6-DCQ epoxide → 2,6-DCQOH	−95.2 → −94.8	−0.4
2,6-DCQ epoxide + H_2O → CQ-diOH + HCl	−143.1 → −138.9	+4.2

[a] The base-catalyzed pathway is the nonphotochemical pathway observed in this study. The H_2O_2 addition to form epoxide is primarily a photochemical pathway.

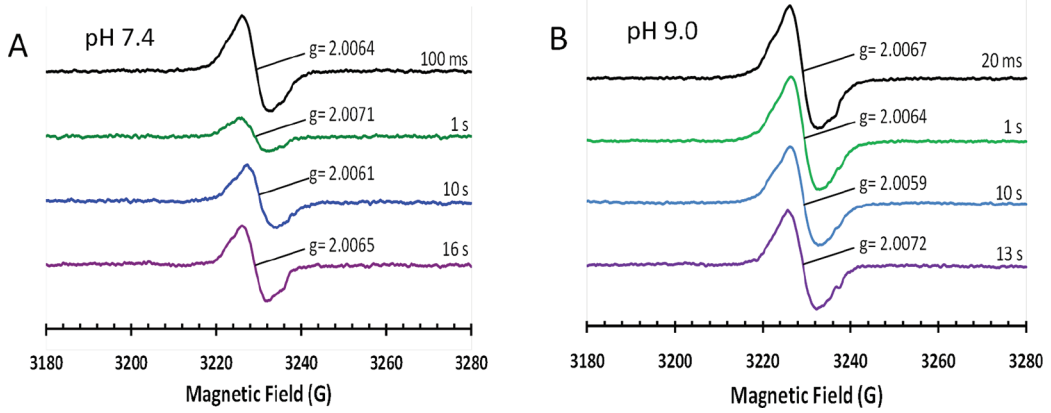

Figure 9. ESR spectra of the reaction mixture of H_2O_2 with 2,6-DCQ at pH 7.4 (A) and 9.0 (B). Rapid-freeze-quench samples (100 ms, 1 s, and 10 s) were prepared from the reaction of H_2O_2 (final concentration of 0.25 mM) with 2,6-DCQ (final concentration of 0.25 mM) at 20 °C and rapidly frozen in an isopentane slurry. The samples quenched at 16 and 13 s (A and B) were prepared using manual mixing. Spectra were recorded at 190 K using the spectrometer settings described in the Experimental Section. The frequency of the experiments was 9.0698 and 9.0699 GHz in panels A and B, respectively.

possible outcomes for the 2,6-DCQ diOH intermediate. The minor pathway consists of the elimination of HCl to form CQ-DiOH with a net free energy change of $\Delta G^{\circ}_{\text{CQ diOH}} = +4.2$ kJ/mol. The major pathway is the elimination of H_2O to form 2,6-DCQOH with $\Delta G^{\circ}_{\text{2,6-DCQOH}} = -0.4$ kJ/mol. These calculations were carried out in a vacuum. It is anticipated that inclusion of solvent would make the free energy for product formation more favorable. The free energy considerations suggest that 2,6-DCQOH would be the favored product at low pH, although the accuracy of the method is not greater than 4 kJ/mol so that it is possible that the dihydroxy compound, 2,6-DCQ diOH, is formed as well. The numerical values for each intermediate and product are presented in Table 1.

DISCUSSION

The present study confirms that 2,6-DCQOH is the major product of the nonphotochemical base-catalyzed oxidation of 2,6-DCQ. This observation builds on previous work showing that the formation of 2,6-DCQ is the primary product of the catalytic oxidation of 2,4,6-TCP catalyzed by DHP A and B and cosubstrate H_2O_2 by a one-electron mechanism.[24] Evidence suggests that both the catalytic transformation leading to 2,6-DCQ formation and the ensuing spontaneous hydroxylation reaction occur by a radical mechanism. Radical formation is thus a pervasive feature of catalytic oxidation of 2,4,6-TCP and similar halogenated phenols, which likely is related to the toxicity of these molecules. While phenoxyl radicals have been discussed in a number of studies, the central role played by quinone radicals, revealed by this study, is likely to have a significant consequence in *A. ornata*, as well as for any development of DHP A and B for biotechnology applications.

Radical chemistry is important for all aspects of oxidation of 2,4,6-TCP and related phenolic compounds by peroxidases. Following the cloning and expression of DHP A,[3] we pointed out that if the substrate binds internally, as originally proposed,[12] then a one-electron oxidation mechanism would require a radical product, a phenoxyl radical, to diffuse through the protein.

dx.doi.org/10.1021/jp208536x |J. Phys. Chem. B 2012, 116, 1666–1676

Given the high reactivity of phenoxyl radicals, there would be a significant possibility of radical reactions as this radical would pass by tyrosines 28, 34, and 38 on its migration toward the solvent. Consistent with this concern, we have shown that tyrosine radicals are observed with nearly 100% yield in DHP A when substrate is not present.[25,26] We have recently confirmed that 2,4,6-trichlorophenoxyl radicals can be directly observed following oxidation of 2,4,6-TCP by DHP.[23] To resolve the paradox of radical reactivity at an internal site, we suggested that a two-electron oxidation could be a reasonable mechanism to explain an internal substrate binding site.[12] However, the hypothesis that the internal site was a substrate binding site was disproven by inhibition studies combined with resonance Raman spectroscopy that showed opposing effects of inhibitor 4-BP and substrate 2,4,6-TCP on the distal histidine (H55) conformation.[14] Furthermore, NMR data clearly showed different patterns of interaction for inhibitors, such as 4-BP, and substrates, such as 2,4,6-TCP, which suggested internal and external modes of binding, respectively.[15,16] We have also shown that phenoxyl radical (2,4,6-TCPO$^{\bullet}$) dismutation is rapid, such that it can only be observed by flow-ESR.[23] The observed product in spectrophotometric assays is 2,6-DCQ, which has a maximum absorbance at 273 nm.[24,26] Thus, we currently understand the mechanism of substrate oxidation to involve external binding of 2,4,6-TCP followed by one electron oxidation to form the 2,4,6-TCPO$^{\bullet}$ radical followed by radical dismutation. The oxidized 2,4,6-TCP cation rearranges to form 2,6-DCQ and Cl^-.

Our study finds significant nonphotochemical reactivity of 2,6-DCQ via a radical mechanism that has not been previously described. We have correlated the decline in product, 2,6-DCQ, concentration at 273 nm with the appearance of 2,6-DCQOH (λ_{max} = 524 nm, ε = 2350 M^{-1} cm^{-1}) (Figures S4 and S5) using studies to show both temperature and pH-dependence. Although we have relied on DHP A for the mechanistic comparisons that involve enzymatic catalysis, it is believed that the spontaneous hydroxylation chemistry has general validity for all peroxidases, and indeed for any process that produces 2,6-DCQ. While the observed spectral changes are consistent with hydroxylation of 2,6-DCQ, the hypothesis of a secondary product requires a structural proof. We have used 2D $^1H-^{13}C$ HMBC NMR experiments to establish the identity of the secondary product, 2,6-DCQOH. We were compelled to use DMSO as a solvent for these studies due to the low solubility of 2,6-DCQ in aqueous solution. The addition of H_2O_2 to 2,6-DCQ in DMSO provides firm evidence that 2,6-DCQOH is the major species formed by the spontaneous oxidation of 2,6-DCQ.

The temperature dependence of the reaction confirms the kinetic model for the formation of the hydroxylated product. Specifically, it explains why 2,6-DCQOH is observed in significant yield only when the temperature exceeds 20 °C. The nonphotochemical hydroxylation of 2,6-DCQ has a measurable rate above 10 °C. The kinetics of the 2,6-DCQ product formation and decay by the nonphotochemical hydroxylation reaction have a biexponential form above 25 °C. The fit to an Arrhenius model associated with the Michaelis−Menten kinetic scheme gave an activation energy of $E_a \approx 56$ kJ/mol for substrate oxidation to form 2,6-DCQ.[24] This activation barrier was hypothesized to be primarily due to the requirement for substrate diffusion to the active site on the surface of DHP A, which was the rate-limiting process in the complex peroxidase reaction scheme.[24] The data presented here show that 2,6-DCQOH has a significantly lower activation energy of $E_a \approx 36$ kJ/mol for the hydroxylation of 2,6-DCQ to form 2,6-DCQOH (Arrhenius plot in Table S2 and Figure S3). This activation energy is consistent with DFT calculations that show that the initial hydroxylation step has a free energy of 41 kJ/mol (Table 1), which would suggest that attack by hydroxide is the rate-limiting step in the formation of 2,6-DCQOH at pH 7.4 and hence explains the activation barrier. However, the relative activation energies of the two processes, formation of 2,6-DCQ and 2,6-DCQOH, do not explain why the hydroxylation is observed first above 20 °C. The empirical fact that the rate of formation of 2,6-DCQOH increases more rapidly than the catalyzed rate of 2,6-DCQ formation as a function of temperature shown in Figure 6 can be modeled as a pseudofirst-order process as described in the Supporting Information. The justification for a pseudofirst-order treatment is that concentrations of enzyme (DHP A), H_2O_2, and OH^- are essentially constant on the time scale of the reaction. This simplifying assumption can explain the temperature dependence of formation of 2,6-DCQ and subsequent formation of 2,6-DCQOH. The ∼36 kJ/mol activation energy for the intrinsic rate constant for the hydroxylation reaction means that it decreases by a factor ∼2 between 15 and 30 °C. The temperature dependence of the formation of 2,6-DCQ is greater, and it changes by ∼3.5 over this range. Thus, even though the temperature dependence of the hydroxylation reaction is smaller than that of the formation, the time scale for that process shifts from ∼100 s at 30 °C to ∼300 s at 15 °C for the observable onset of 2,6-DCQOH formation. Because our kinetic analyses were conducted for 300 s, we did not observe a significant decay of 2,6-DCQ at temperatures below 20 °C. The kinetic model calculated from the rate equations based on a finite difference approach presented in Figures S8−S10 explains the appearance of the data at both 273 and 524 nm.

At low pH, the oxidation of 2,6-DCQ may occur by H_2O_2 epoxidation of the quinone (Scheme 1). The epoxide could be ring opened to form either the trans or the cis diols in aqueous solution. There are then two possible mechanisms leading to distinct products. First, the elimination of HCl and formation of CQ-DiOH is possible. The second mechanism, involving the elimination of H_2O leading to the formation of 2,6-DCQOH, is the favored reaction based on the DFT calculations. The photochemistry of 2,6-DCQ appears to be more complex than was previously thought based on the observation of radicals in the RFQ-ESR and reactivity even in the absence of H_2O_2 as shown in Figure S13. We note that the epoxidation mechanism does not occur via a radical mechanism and would be ESR-silent. The UV−vis data in Figure S13 may contain a contribution from this pathway. The ESR data in Figures S11 and S12 suggest that photochemistry can affect the radical pathway at higher pH. These facts are mentioned in this report for the sake of completeness, although we make no claim to have conducted a comprehensive study of the photochemical pathway. The photochemical pathway is worth including in our discussion because there clearly is relevance to the biological degradation of 2,4,6-TBP and 2,4,6-TCP. The nonphotochemical yield of hydroxylation product falls nearly to zero by pH 5, which strongly suggests that base catalysis is required for nonphotochemical reactivity in the presence of H_2O_2.

This study validates the hypothesis that a base-catalyzed radical-mediated process is responsible for the nonphotochemical oxidation of 2,6-DCQ. The base-catalyzed reaction may also involve reactivity by HOO^- at high pH. Attack by OH^- yields HQ2 and radical intermediates, SQ1 and SQ2, that can form 2,6-DCQOH and regenerate 2,6-DCQ as shown in Scheme 3.

The data obtained at pH 7.4 showing the transient concentration of two radicals are readily explained by the mechanism shown in Schemes 2 and 3. Scheme 1 provides a plausible mechanism for the base-catalyzed hydroxylation of 2,6-DCQ in aqueous solution at pH 7.4. 2,6-DCQ can undergo base-catalyzed nucleophilic addition leading to HQ2. Product HQ2 is a hydroquinone dianion, which can be involved in a cross-oxidation reaction with 2,6-DCQ to yield the observed semiquinone radicals, SQ1 and SQ2 (Scheme 2). Semiquinone SQ2 can react with 2,6-DCQ to yield SQ1 and the hydroxylated product, 2,6-DCQ-3-OH (Scheme 2). On the basis of the mechanism in Scheme 2, which leads to HQ2 and subsequent formation of semiquinone radicals, OH^- is thought to dominate at pH 7.4, even though the $[OH^-]$ and $[HOO^-]$ concentrations are nearly equal at this pH. We note that $[OH^-] = 2.5 \times 10^{-7}$ M at pH 7.4 as compared to $[HOO^-] = 3.0 \times 10^{-7}$ M for $[H_2O_2] = 500\ \mu$M. The latter is based on the pK_a of 11.6 for H_2O_2, a reaction pH of 7.4, and the Henderson−Hasselbach equation rearranged to give $[HOO^-] = [H_2O_2]10^{pH-pK_a}$. On the basis of RFQ-ESR, we have also found that there is an additional base-catalyzed photochemical reaction, which may yield a dihydroxylated product, 2,6-dichloro-3,5-dihydroxyquinone, shown in Scheme S1 of the Supporting Information. The RFQ-ESR data showing the radicals produced under those conditions are given in Figures S11 and S12.

Finally, we consider the high pH mechanism and the observation that no radical signal was observed in room-temperature benchtop mixing experiments at pH 9.0, and yet radicals were detected under RFQ-ESR conditions. At pH 9.0, $[HOO^-] = 1.2 \times 10^{-6}$ M and $[OH^-] = 10^{-5}$ M, which would also suggest formation of HQ2. However, the HPLC data show that the reaction is an order of magnitude more rapid at this pH. The fact that no radical was observed in the ESR spectrum obtained in benchtop mixing ESR experiments at room temperature suggests two possibilities. First, it is possible that the reaction is so much faster that no radicals are observed under rapid mixing conditions. The time constant for formation of 2,6-DCQOH is less than 1 min at pH 9.0, whereas it is ∼10 min at pH 7.4. A second possibility is a direct nucleophilic attack by HOO^- at pH 9. As shown in Scheme 1, this mechanism could potentially generate the 2,6-DCQOH product without forming radicals. Because radicals are observed by RFQ-ESR at pH 9, we favor the first possibility and include the second one for completeness. The conclusions reached in this study show how the flow and rapid-freeze quench ESR data complement each other. The assignment of the radicals would have been difficult using the RFQ-ESR technique. However, the kinetic trajectory of radical formation and reaction is not discernible from flow ESR alone.

CONCLUSION

For both applied and fundamental reasons, it is valuable to understand the mechanism of oxidation of 2,4,6-TCP to 2,6-DCQ by DHP. Chlorophenols, which have been produced industrially on a large scale, constitute a significant class of environmental pollutants.[61−63] Specifically, 2,4,6-TCP has been used extensively as wood preservatives and pesticides.[64] 2,4,6-TCP is also useful as a model substrate in DHP A and B, because it has close structural similarity to 2,4,6-TBP, the native substrate of DHP, and is more soluble. The present study demonstrates that 2,6-DCQOH is a spontaneous oxidation product of 2,6-DCQ formed during the catalytic oxidation of 2,4,6-TCP by DHP. This work shows that the secondary hydroxylation reaction is significant at physiological temperatures and pH, which suggests that 2,6-DCQOH is an important intermediate in the degradation of 2,4,6-TCP in benthic ecosystems where *A. ornata* is found, as well as in any bioremediation process designed to use DHP A or B. The study focused on the nonphotochemical process, which occurs at physiological pH. However, we have also shown that this set of oxidation reactions is even more complex and that a complete study would have to include temperature, pH, H_2O_2 concentration, and light flux as variables that would be studied by flow and rapid-freeze-quench ESR as key methods to elucidate the pathways.

ASSOCIATED CONTENT

Supporting Information. Table S1: Predicted and experimental chemical shifts. Figure S1: Calculation of initial rates for formation of 2,6-DCQ and 2,6-DCQOH. Figure S2: HSQC data for 2,6-DCQ and 2,6-DCQOH. Figure S3: Single wavelength (524 nm) kinetic trace of 2,6-DCQOH. Figure S4: The biexponential kinetics of 2,6-DCQ formation. Figure S5: The exponential growth of the secondary product, 2,6-DCQOH, at 524 nm. Figure S6: Study of the hydroxylation of 2,6-DCQ at different temperatures. Table S2: Rate constants for hydroxylation of 2,6-DCQ at different temperatures. Figure S7: Arrhenius plot of the data fit to the model equation. Figure S8: Calculated model for kinetics at 30 °C. Figure S10: Calculated model for kinetics at 15 °C. Figure S19: Comparison of kinetics calculated at 30 and 15 °C. Figure S10: ESR spectra of 2,6-DCQ with added H_2O_2 at pH 7.4. Figure S11: ESR spectra of 2,6-DCQ with added H_2O_2 at pH 9. Figure S12: UV−vis spectra of the reaction of 2,6-DCQ with and without H_2O_2. Scheme S1: Possible model for a second hydroxylation. This material is available free of charge via the Internet at http://pubs.acs.org.

AUTHOR INFORMATION

Corresponding Author
*Tel.: (919) 515-8915. E-mail: stefan_franzen@ncsu.edu.

ACKNOWLEDGMENT

R.G. and S.F. gratefully acknowledge support by Army Research Office Grant 57861-LS. We gratefully acknowledge the receipt of a PUC-19 plasmid containing the eukaryotic DHP A gene from Drs. Lincoln and Dawson of the University of South Carolina.

REFERENCES

(1) Ferrari, R. P.; Laurenti, E.; Trotta, F. *JBIC, J. Biol. Inorg. Chem.* **1999**, *4*, 232–237.
(2) Laurenti, E.; Ghibaudi, E.; Ardissone, S.; Ferrari, R. P. *J. Inorg. Biochem.* **2003**, *95*, 171–176.
(3) Belyea, J.; Gilvey, L. B.; Davis, M. F.; Godek, M.; Sit, T. L.; Lommel, S. A.; Franzen, S. *Biochemistry* **2005**, *44*, 15637–15644.
(4) Franzen, S.; Gilvey, L. B.; Belyea, J. L. *Biochim. Biophys. Acta, Proteins Proteomics* **2007**, *1774*, 121–130.
(5) Franzen, S.; Belyea, J.; Gilvey, L. B.; Davis, M. F.; Chaudhary, C. E.; Sit, T. L.; Lommel, S. A. *Biochemistry* **2006**, *45*, 9085–9094.
(6) Osborne, R. L.; Coggins, M. K.; Raner, G. M.; Walla, M.; Dawson, J. H. *Biochemistry* **2009**, *48*, 4231–4238.
(7) Osborne, R. L.; Coggins, M. K.; Walla, M.; Dawson, J. H. *Biochemistry* **2007**, *46*, 9823–9829.
(8) Chen, Z.; de Serrano, V.; Betts, L.; Franzen, S. *Acta Crystallogr., Sect. D: Biol. Crystallogr.* **2009**, *D65*, 34–40.

(9) de Serrano, V.; Chen, Z.; Davis, M. F.; Franzen, S. *Acta Crystallogr., Sect. D: Biol. Crystallogr.* **2007**, *D63*, 1094–1101.
(10) de Serrano, V.; D'Antonio, J.; Franzen, S.; Ghiladi, R. A. *Acta Crystallogr., Sect. D: Biol. Crystallogr.* **2010**, *66*, 529–538.
(11) de Serrano, V. S.; Davis, M. F.; Gaff, J. F.; Zhang, Q.; Chen, Z.; D'Antonio, E. L.; Bowden, E. F.; Rose, R.; Franzen, S. *Acta Crystallogr., Sect. D: Biol. Crystallogr.* **2010**, *66*, 770–782.
(12) Lebioda, L.; LaCount, M. W.; Zhang, E.; Chen, Y. P.; Han, K.; Whitton, M. M.; Lincoln, D. E.; Woodin, S. A. *Nature (London)* **1999**, *401*, 445.
(13) LaCount, M. W.; Zhang, E.; Chen, Y. P.; Han, K.; Whitton, M. M.; Lincoln, D. E.; Woodin, S. A.; Lebioda, L. *J. Biol. Chem.* **2000**, *275*, 18712–18716.
(14) Thompson, M. K.; Davis, M. F.; deSorrano, V.; Nicoletti, F. P.; Howes, B. D.; Smulevich, G.; Franzen, S. *Biophys. J.* **2010**, *99*, 1586–1595.
(15) Davis, M. F.; Bobay, B. G.; Franzen, S. *Biochemistry* **2010**, *49*, 1199–1206.
(16) Davis, M. F.; Gracz, H.; Vendeix, F. A. P.; de Serrano, V.; Somasundaram, A.; Decatur, S. M.; Franzen, S. *Biochemistry* **2009**, *48*, 2164–2172.
(17) Nienhaus, K.; Deng, P.; Belyea, J.; Franzen, S.; Nienhaus, G. U. *J. Phys. Chem. B* **2006**, *110*, 13264–13276.
(18) Nienhaus, K.; Nickel, E.; Davis, M. F.; Franzen, S.; Nienhaus, G. U. *Biochemistry* **2008**, *47*, 12985–12994.
(19) Nicoletti, F. P.; Thompson, M. K.; Howes, B. D.; Franzen, S.; Smulevich, G. *Biochemistry* **2010**, *49*, 1903–1912.
(20) Dunford, H. B. *Xenobiotica* **1995**, *25*, 725–733.
(21) Ator, M. A.; David, S. K.; Demontellano, P. R. O. *J. Biol. Chem.* **1987**, *262*, 14954–14960.
(22) Raven, E. L. *Subcell. Biochem.* **2000**, *35*, 317–349.
(23) Sturgeon, B. E.; Battenburg, B. J.; Lyon, B. J.; Franzen, S. *Chem. Res. Toxicol.*, ASAP.
(24) Ma, H.; Thompson, M. K.; Gaff, J. F.; Franzen, S. *J. Phys. Chem. B* **2010**, *114*, 13823–13829.
(25) Thompson, M. K.; Franzen, S.; Ghiladi, R. A.; Reeder, B. J.; Svistunenko, D. A. *J. Am. Chem. Soc.* **2010**, *132*, 17501–17510.
(26) Feducia, J.; Dumarieh, R.; Gilvey, L. B. G.; Smirnova, T.; Franzen, S.; Ghiladi, R. A. *Biochemistry* **2009**, *48*, 995–1005.
(27) D'Antonio, J.; Ghiladi, R. A. *Biochemistry* **2011**, *50*, 5999–6011.
(28) D'Antonio, J.; D'Antonio, E. L.; Thompson, M. K.; Bowden, E. F.; Franzen, S.; Smirnova, T.; Ghiladi, R. A. *Biochemistry* **2010**, *49*, 6600–6616.
(29) Lente, G.; Espenson, J. H. *Green Chem.* **2005**, *7*, 28–34.
(30) Song, Y.; Buettner, G. R. *Free Radical Biol. Med.* **2010**, *49*, 919–962.
(31) Wong, S. K.; Wan, J. K. S.; Sytnyk, W. *Can. J. Chem.* **1972**, *50*, 3052–&.
(32) Sorokin, A.; Meunier, B.; Seris, J.-L. *Science* **1995**, *268*, 1163–1166.
(33) Xun, L.; Webster, C. M. *J. Biol. Chem.* **2004**, *279*, 6696–6700.
(34) Song, Y.; Wagner, B. A.; Lehmler, H.-J.; Buettner, G. R. *Chem. Res. Toxicol.* **2008**, *21*, 1359–1367.
(35) Fielman, K. T.; Woodin, S. A.; Walla, M. D.; Lincoln, D. E. *Mar. Ecol.: Prog. Ser.* **1999**, *181*, 1–12.
(36) Lincoln, D. E.; Fielman, K. T.; Marinelli, R. L.; Woodin, S. A. *Biochem. Syst. Ecol.* **2005**, *33*, 559–570.
(37) Woodin, S. A.; Lindsay, S. M.; Lincoln, D. E. *Mar. Ecol.: Prog. Ser.* **1997**, *157*, 303–306.
(38) Woodin, S. A.; Walla, M. D.; Lincoln, D. E. *J. Exp. Mar. Biol. Ecol.* **1987**, *107*, 209–217.
(39) Han, K.; Woodin, S. A.; Lincoln, D. E.; Fielman, K. T.; Ely, B. *Mar. Biotechnol.* **2001**, *3*, 287–292.
(40) Chen, Y. P.; Woodin, S. A.; Lincoln, D. E.; Lovell, C. R. *J. Biol. Chem.* **1996**, *271*, 4609–4612.
(41) Gunther, M. R.; Sturgeon, B. E.; Mason, R. P. *Free Radical Biol. Med.* **2000**, *28*, 709–719.
(42) Duling, D. R. *J. Magn. Reson., Ser. B* **1994**, *104*, 105–110.
(43) Perdew, J. P.; Burke, K.; Wang, Y. *Phys. Rev. B: Condens. Matter* **1996**, *54*, 16533–16539.
(44) Andzelm, J.; King-Smith, R. D.; Fitzgerald, G. *Chem. Phys. Lett.* **2001**, *335*, 321–326.
(45) Baker, J.; Kessi, A.; Delley, B. *J. Chem. Phys.* **1996**, *105*, 192–212.
(46) Delley, B. *J. Chem. Phys.* **1990**, *92*, 508–517.
(47) Delley, B. *J. Chem. Phys.* **2000**, *113*, 7756–7764.
(48) Weinert, M.; Davenport, J. W. *Phys. Rev. B* **1992**, *45*, 13709.
(49) Andzelm, J.; Kolmel, C.; Klamt, A. *J. Chem. Phys.* **1995**, *103*, 9312–9320.
(50) Lente, G.; Espenson, J. H. *New J. Chem.* **2004**, *28*, 847–852.
(51) Sorokin, A.; DeSuzzoniDezard, S.; Poullain, D.; Noel, J. P.; Meunier, B. *J. Am. Chem. Soc.* **1996**, *118*, 7410–7411.
(52) Lente, G.; Espenson, J. H. *Chem. Commun.* **2003**, 1162–1163.
(53) (ACD/Laboratories). CAS Registry Number: 89465-84-9; Software V9.07 ed.; Advanced Chemistry Development.
(54) Cook, P. F.; Cleland, W. W. *Biochemistry* **1981**, *20*, 1797–1805.
(55) Zaks, A.; Klibanov, A. M. *Proc. Natl. Acad. Sci. U.S.A.* **1985**, *82*, 3192–3196.
(56) Vitello, L. B.; Huang, M.; Erman, J. E. *Biochemistry* **1990**, *29*, 4283–4288.
(57) Thomas, P. G.; Russell, A. J.; Fersht, A. R. *Nature* **1985**, *318*, 375–376.
(58) Conroy, C. W.; Tyma, P.; Daum, P. H.; Erman, J. E. *Biochim. Biophys. Acta, Protein Struct.* **1978**, *537*, 62–69.
(59) Mermin, D. *Phys. Rev. A* **1965**, *137*, 1441–1443.
(60) Delley, B. *Mol. Simul.* **2006**, *32*, 117–123.
(61) Reddy, G. V. B.; Gelpke, M. D. S.; Gold, M. H. *J. Bacteriol.* **1998**, *180*, 5159–5164.
(62) Duran; Deschler; Precigou; Goulas *Appl. Microbiol. Biotechnol.* **2002**, *59*, 284–288.
(63) Bumpus, J. A.; Aust, S. D. *BioEssays* **1987**, *6*, 166–170.
(64) Hiratsuka, N.; Oyadomari, M.; Shinohara, H.; Tanaka, H.; Wariishi, H. *Biochem. Eng. J.* **2005**, *23*, 241–246.